International Journal of Nanomedicine

Dovepress
open access to scientific and medical research

Open Access Full Text Article

ORIGINAL RESEARCH

Green synthesis of silver nanoparticles by *Chrysanthemum morifolium* Ramat. extract and their application in clinical ultrasound gel

This article was published in the following Dove Press journal:
International Journal of Nanomedicine
6 May 2013
Number of times this article has been viewed

Yan He[1]
Zhiyun Du[1,2]
Huibin Lv[1]
Qianfa Jia[1]
Zhikai Tang[1]
Xi Zheng[1,3]
Kun Zhang[1]
Fenghua Zhao[1]

[1]Institute of Natural Medicine and Green Chemistry, School of Chemical Engineering and Light Industry, Guangdong University of Technology, Guangzhou, People's Republic of China; [2]State Key Laboratory of Natural and Biomimetic Drugs, Peking University, Beijing, People's Republic of China; [3]Susan Lehman Cullman Laboratory for Cancer Research, Department of Chemical Biology, Ernest Mario School of Pharmacy, Rutgers, The State University of New Jersey, Piscataway, NJ, USA

Correspondence: Zhiyun Du
Institute of Natural Medicine and Green Chemistry, School of Chemical Engineering and Light Industry, Guangdong University of Technology, 232 Wai Huan East Road, Guangzhou Higher Education Mega Center, Guangzhou 510006, People's Republic of China
Tel +86 20 3932 2235
Email zhiyundu@gdut.edu.cn

Fenghua Zhao
School of Chemical Engineering and Light Industry, Guangdong University of Technology, 232 Wai Huan East Road, Guangzhou Higher Education Mega Center, Guangzhou 510006, People's Republic of China
Tel +86 20 3932 2203
Email seazhaofh@163.com

Abstract: Eco-friendly green synthesis with plant extracts plays a very important role in nanotechnology, without any harmful chemicals. In this report, the synthesis of water-soluble silver nanoparticles was developed by treating silver ions with *Chrysanthemum morifolium* Ramat. extract at room temperature. The effect of the extract on the formation of silver nanoparticles was characterized by ultraviolet and visible absorption spectroscopy, X-ray diffraction, transmission electron microscopy, and Fourier transform infrared spectroscopy. The ultraviolet and visible absorption spectroscopy results show a strong resonance centered on the surface of silver nanoparticles (AgNP) at 430 nm. The Fourier transform infrared spectroscopy spectral study demonstrates *Chrysanthemum morifolium* Ramat. extract acted as the reducing and stabilizing agent during the synthesis. The X-ray diffraction analysis confirmed that the synthesized AgNP are single crystallines, corresponding with the result of transmission electron microscopy. Water-soluble AgNP, with an approximate size of 20 nm–50 nm were also observed in the transmission electron microscopy image. The bactericidal properties of the synthesized AgNP were investigated using the agar-dilution method and the growth-inhibition test. The results show the AgNP had potent bactericidal activity on *Staphylococcus aureus* and *Escherichia coli*, as well as a strong antibacterial activity against gram-negative bacteria, as compared to gram-positive bacteria with a dose-dependent effect, thus providing a clinical ultrasound gel with bactericidal property for prevention of cross infections.

Keywords: silver nanoparticles, green synthesis, *Chrysanthemum morifolium* Ramat., bactericidal activity, ultrasound gel

Introduction

Over the past few decades, noble-metal nanoparticles expanded rapidly with the incorporation of new nanocomposites into a range of products and technologies. Silver nanoparticles are the most sought-after functionalizing and commercializing nanomaterial due to their unique physicochemical properties (with a high ratio of surface area to mass), electric,[1] optical,[2] catalytic,[3] and particularly antimicrobial properties.[4] The nanoparticles showed potent antibacterial activity and a significantly higher synergistic effect with erythromycin, methicillin, and ciprofloxacin.[5] Silver nanoparticles are also reported to possess antifungal,[6] anti-inflammatory,[7] antiviral,[8] anti-angiogenesis,[9] and antiplatelet[10] activities. They all confer to them a major advantage for the development of alternative products against, for example, multidrug-resistant microorganisms.[11] Silver nanoparticles (AgNP), as antibacterial agents, are now used extensively in the fields of medicine,[12] implantable biomaterial,[13] water treatment,[14] molecular imaging,[15] diagnosis and treatment of cardiovascular diseases,[16] wound healing,[17] drug delivery,[18] and clothing.[19]

Synthesis of nanoparticles is presently an important area of research, searching for an eco-friendly manner and green materials for current science. A number of AgNP have been developed by a chemical approach, a physical approach, and a recently developed biological method.[20] The latter has emerged as a green alternative, for it is environment-friendly, cost-effective, and easily scaled-up. It has great potential with natural reductants,[21,22] such as plants' extract,[23] bacteria,[24] and fungus.[25] Plant extracts are more advantageous because using them eliminates the elaborate process of maintaining cell cultures and can be suitably scaled-up for large-scale production under nonaseptic environments. Especially plants that secrete the functional molecules for the reaction, compatible with the green chemistry principles. There are some examples of synthesizing nanomaterial using plants, such as *Camellia sinensis*,[26] *Sesuvium portulacastrum L.*,[27] and *marine polysaccharide*.[28]

Chrysanthemum morifolium Ramat. has been widely used in the People's Republic of China as a health food and medicine for thousands of years.[29] It has various biological features, including anti-inflammation,[30] antioxidant activity,[31] cardiovascular protection,[32] antitumorigenesis,[33] anti-HIV,[34] and anti-aging activities.[35] It contains a wide variety of flavonoids,[36] caffeoylquinic acids,[37] chlorogenic acid,[38] phenolic acids,[39] etc, which could be used as reductants to react with silver ions and as scaffolds to direct the formation of AgNP in solution.

Nosocomial infections are posing an increasingly serious problem in the hospital setting in current years.[40] With the increasing use of ultrasound in medical diagnosis and adjuvant therapies, there is the potential for the transmission of nosocomial infections via the ultrasound transducer and coupling gel.[41] In the present work, we have proposed for the first time the results of a green synthesis method for AgNP, using *Chrysanthemum morifolium* Ramat. extract as a reducing and stabilizing agent. This work has been conducted to develop a cost-effective preparation method of AgNP at room temperature and in short-reaction time. Also, we have investigated the bactericidal activity of the synthesized AgNP against *Staphylococcus aureus* and *Escherichia coli*. Furthermore, this paper provides a simple and eco-friendly strategy for developing a novel clinical ultrasound gel with bactericidal property for prevention of cross infections.

Materials and methods

Materials

Chrysanthemum morifolium Ramat. (CM), sourced from the Zhejiang province in the People's Republic of China, was purchased from a local drugstore in Guangzhou, People's Republic of China, and identified as dry flowers of CM by our team member. Silver nitrate ($AgNO_3$) was purchased from Sigma-Aldrich, St Louis, MO, USA. Double-distilled deionized water was used to perform the experiments. Poly acrylic acid, glycerine and NaDH from Baishi (Tianjin, People's Republic of China). *S. aures* and *E. coli* were offered by Guangdong Institute of Microbiology (Guanzhou, People's Republic of China).

Synthesis of AgNP

Dried CM flowers were washed three times with distilled water to remove dirt and soil. Next, 20 grams of flowers were immersed in 300 mL boiling distilled water for 10 minutes. The cooled filtrate obtained was stored at 4°C for further use. The 50 mL of $AgNO_3$ (2 mmol/L) aqueous solution was reacted with 50 mL drops of the obtained extract solutions in a flask with stirring for 30 minutes and then continued stirring for 24 hours at room temperature.

Characterization of AgNP

The optical property of prepared Ag nanoparticles was analyzed via ultraviolet and visible absorption spectroscopy (TU1900, Persee, Beijing, People's Republic of China) absorption double-beam spectrophotometer with a deuterium and tungsten iodine lamp in the range from 300 nm–800 nm at room temperature. Phase formation of the synthesized nanoparticles was characterized by X-ray diffraction. Diffraction data for thin thoroughly dried nanoparticle films on glass slides were recorded on an X-ray diffractometer (Ultima III, Rigaku, Tokyo, Japan) with $Cu_{k\alpha}$ radiation ($\lambda = 1.5406$ Å) source in the 2θ range of 10°–80° with 4°/minute scanning rate. The functional group and composition of AgNP were characterized by Fourier transform infrared (Nicolet 380™, Thermo Electron, MA, USA) spectroscopy in the range of 4000 cm–500 cm^{-1}.

The surface morphology, shape and size of the prepared AgNP were observed by a transmission electron microscope (TEM), (JEM-2010HR, JEOL, Tokyo, Japan). The morphology and size of the AgNP were also characterized by a higher resolution transmission electron microscope (HRTEM, JEM-2010HR, JEOL). The nanoparticles were added on a carbon-coated copper grid, and the examinations were operated at 200 kv.

Bactericidal activities of AgNP

The bactericidal activity of AgNP was tested against *S. aureus* (ATCC6538) and *E. coli* (ATCC25922) using an agar-dilution

method and growth-inhibition test on Mueller–Hinton agar plates (Tianhe, Hangzhou, People's Republic of China).[42] The plates were supplemented with various concentrations of AgNP (from 0 μg/mL–20 μg/mL), and each plate was inoculated with 1.0×10^7 colony-forming units (CFU) of bacteria by spread plating. Plates without AgNP were used as control. After 18 hours incubation at 37°C, plates were observed for bacterial colony formation. To test bacteria growth inhibition by AgNP, 180 μL of *S. aureus* or *E. coli* suspension with 1.0×10^8 CFU was inoculated into 30 mL volumes of fresh luria bertaini (LB) media with concentrations of 0, 2.5, 5, 10, and 20 μg/mL AgNP, respectively. During an aerobic incubation at 37°C, the optical densities at 600 nm (OD600) of the cultures were determined using a ultraviolet-visible spectrophotometer (TU1900, Persee, Beijing, People's Republic of China).

Preparation of clinical ultrasound gel containing AgNP

The ultrasound gel containing 10 μg/mL AgNP was prepared, based on the bactericidal activity of the AgNP. The 0.5 grams polyacrylic acid was dispersed in 97.5 mL distilled water with vigorously stirring until it dispersed completely, and then 2.0 grams glycerin and synthesized AgNP solution were added. Diluting NaOH (4.0 MoL/mL) was used to neutralize polyacrylic acid and to control the pH value to 6.5–7.5.

Sterilization of probe of B-ultrasound instrument

The ultrasound gel was placed on the probe of the B-ultrasound instrument and scanned on the abdomen skin of each patient for 5 minutes. Then, the surface of the probe was swabbed and cultured. A total of 50 specimens using commercial ultrasound gel and 50 specimens using self-prepared AgNP ultrasound gel before the cleaning of the probe were analyzed for bacterial contamination with *S. aureus* (ATCC 6538), *E. coli.* (ATCC 8099), *P. aeruginosa.* (ATCC 15442), and *C. albicans* (ATCC 10231). All bacteriologic samples were collected by a single operator with a sterile swab, which was run along the entire surface of the probe. The samples were inoculated on chocolate agar plates (Huasin, Guangzhou, People's Republic of China) and incubated aerobically at 36°C for 48 hours. Colonies were counted at 48 hours. Results were expressed in colony-forming units. Probes were considered sterile when they contained less than 10 colony-forming units. In addition, the image quality of the ultrasound using commercial ultrasound gel and self-prepared AgNP gel was evaluated in the preliminary trial.

Results and discussion

The color change was noted by visual observation in the bottles that contained $AgNO_3$ solution with extract. The color of the $AgNO_3$/extract solution changed from colorless to light yellow and, eventually, to yellow brown. This color change indicates the formation of AgNP in the solution. Extract without $AgNO_3$ did not show any color changes. The formation of AgNP was further confirmed by using ultraviolet-visible spectroscopy (UV-vis), X-ray diffraction (XRD), Fourier transform infrared spectroscopy, transmission electron microscopy, and the high-resolution transmission electron microscopy.

The UV-vis spectroscopy is an indirect method to examine the bioreduction of AgNP from aqueous $AgNO_3$ solution. Figure 1 shows the UV-vis absorption spectrum of the CM extract and synthesized AgNP. The AgNP has the surface plasmon resonance absorption band with free electrons, due

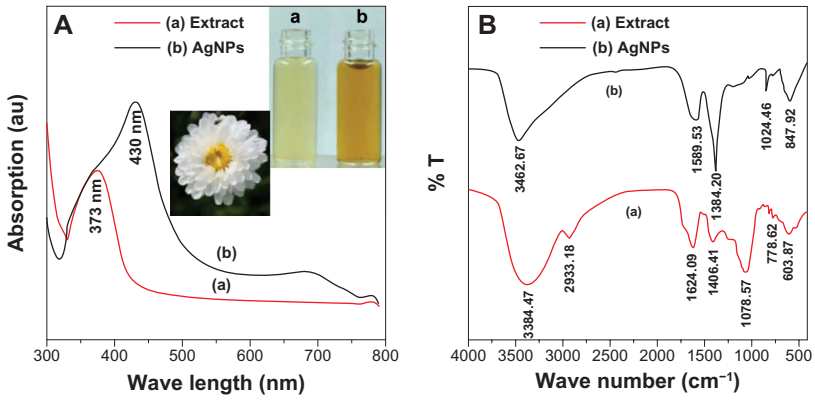

Figure 1 UV-vis and FTIR spectrums of silver nanoparticles and extracts. (**A**) UV-vis and (**B**) FTIR spectrums of silver nanoparticles and extracts, with the inset of the bottle (**a**) of extract and the bottle (**b**) of silver nanoparticles.

Abbreviations: AgNP, silver nanoparticles; au, arbitrary unit; UV-vis, ultraviolet and visible absorption spectroscopy; FTIR, Fourier transform infrared spectroscopy; arb, arbitrary; T, transmission.

to the combined vibration of electrons of AgNP in resonance with a light wave. A broad absorption peak was observed at 430 nm, which is a characteristic band for the Ag, arising from the excitation of longitudinal plasmon vibrations of AgNP in the solution.[30] The absorption peak of the CM extract was observed at 373 nm, which is typical of the absorptions of flavonoids. Flavonoids, such as luteolin-7-*O*-β-D-glucoside and apigenin-7-*O*-β-D-glucoside, are the main components of CM extract.[30] Therefore, the flavonoids of CM extract may play the key roles, not only to reduce the $AgNO_3$ solution to AgNP, but also to stabilize the nanoparticles in the solution.

The Fourier transform infrared spectroscopy (FTIR) measurement was studied to identify the possible biomolecules responsible as capping and reducing agent for the AgNP synthesized by extract (Figure 1B). The intense broad band at 3384 cm^{-1} is due to the O–H stretching mode and at 2921 cm^{-1} due to the aldehydic C–H stretching mode. The peak at 1078 cm^{-1}, which is absent for the AgNP FTIR spectrums, is the bending vibration of the C–O stretch and could be due to the stabilization of AgNP through this group. The peak of C=C group (at 1406 cm^{-1}) absent for AgNP is possible, due to the reduction of $AgNO_3$ to Ag.[43] It is corresponding to the results of the UV-vis spectroscopy that the CM extract played a role as the reducing and stabilizing agent in the preparation of AgNP. This indicated the presence of extracts as a capping agent for AgNP, which increases the stability of the nanoparticles synthesized.

Figure 2 depicts the typical XRD and transmission electron microscopy/high-resolution transmission electron microscopy micrographs of AgNP. Figure 2A shows XRD patterns for AgNP synthesized by extracts. Four main characteristic diffraction peaks for Ag were observed at 2θ = 38.4, 43.3, 64.6, 77.7, which correspond to the (111), (200), (220), and (311) based on the band for face-centered cubic structures of silver, respectively (JCPDS Card Number 87-0717). No peaks from any other phase were observed showing that single-phase Ag with cubic structure nanoparticles has been obtained directly. In general, the width of XRD peaks is related to crystallite size. The Debye–Scherrer equation was used to determine average crystallite diameter from half width of the diffraction peaks:

$$D = (k\lambda)/(\beta \cos \theta) \quad (1)$$

where D is mean crystallite size of the powder; λ is the wavelength of $Cu_{k\alpha}$; β is the full width at half-maximum; θ is the Bragg diffraction angle; and k is a constant. The (111) plane was chosen to calculate crystalline size. From the Debye–Scherrer equation, the average crystallite size of AgNP synthesized is found to be 27.2 nm.

The TEM/HRTEM image of AgNP is shown in Figure 2B. The image shows that the morphology of the AgNP was spherical with an average size of 20 nm–50 nm, which is in good agreement with the particle size calculated from XRD analysis. The interplanar distance calculated from the HRTEM image (Figure 2B inset) is about 0.236 nm, which corresponds to the d-spacing of the (111) planes of cubic Ag.

Antimicrobial activity of the synthesized AgNP was studied, using AgNP on *S. aureus* and *E. coli* at different concentrations of 0, 2.5, 5, 10 μg/mL (Figure 3A). The AgNP, at a concentration of 2.5 μg/mL, was able to inhibit both strains of the bacteria's growth to some extent with fewer bacterial colonies formed on these plates, compared to the bacterial lawn present in the control plates. The AgNP,

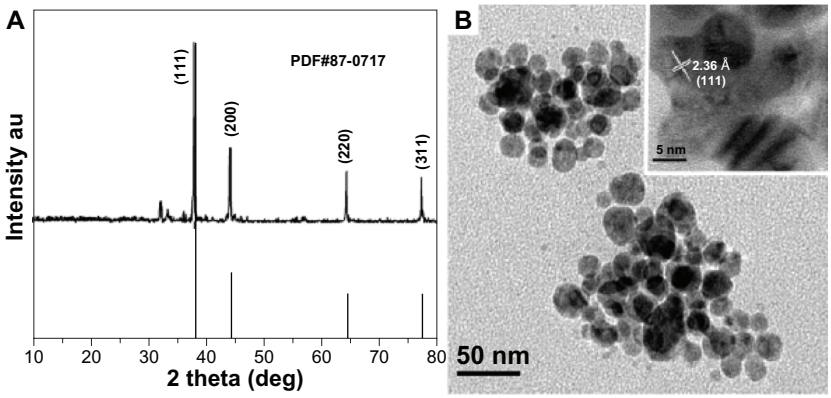

Figure 2 XRD and TEM images of silver nanoparticles. (**A**) XRD and (**B**) TEM images of silver nanoparticles.
Note: HRTEM image is inset in Figure 2B.
Abbreviations: deg, degrees; XRD, X-ray diffraction; TEM, transmission election microscopy; HRTEM, high-resolution transmission electron microscopy; au, arbitrary unit.

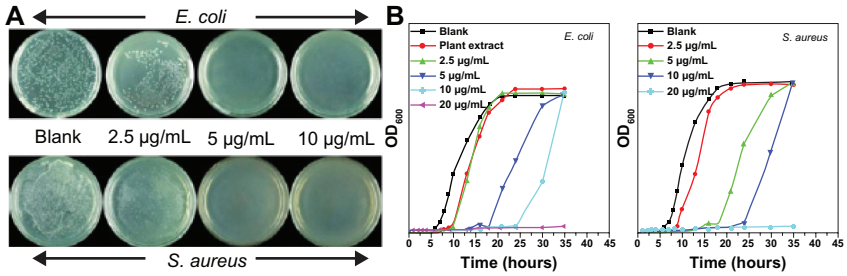

Figure 3 Representative photographs of bactericidal activity of silver nanoparticles at different concentrations. Photographs depict bactericidal activity of silver nanoparticles at different concentrations against (**A**) *E. coli* and *S. aureus* and (**B**) bacterial growth curve of *E. coli* and *S. aureus* in LB media with different concentrations of silver nanoparticles.
Abbreviations: LB, luria-bertani; OD, optical density.

at concentrations of 5 μg/mL and 10 μg/mL, completely killed *S. aureus* and *E. coli*, which is very clearly visualized from the complete absence of colony formation in the plates. Figure 3B shows the effect of AgNP on the growth inhibition of *S. aureus* and *E. coli*. The synthesized AgNP, at concentrations of 5 μg/mL, 10 μg/mL, and 20 μg/mL, can achieve a good antimicrobial activity, while the growth of both *S. aureus* and *E. coli* were completely inhibited in 35 hours at 20 μg/mL, 24 hours at 10 μg/mL, and 16 hours at 5 μg/mL.

Many different researches were carried out on the cytotoxicity effect of medically relevant AgNP. However, different research showed their varying activities largely attributing to preparation methodologies, concentration, and particle size.[45–49] Studies have shown that AgNP showed significant cytotoxicity and affected normal cell proliferation with a large number of cell necrosis at 50 μg/mL and above,[44,45] slightly toxic to cells at 25~50 μg/mL and no longer cytotoxic at 25 μg/mL and lower concentration.[45] Therefore, the safe concentration of AgNP should be less than 25 μg/mL. AgNP at 1 part per million or lower did not show genotoxicity, acute toxicity and intracutaneous reactivity, and exerted effective antimicrobial activities on both the gram (−) and (+) bacterial strains within the range from 0.06 parts per million to 0.98 parts per million for 50% minimum inhibitory concentration (MIC).[46] The smallest-sized AgNP (10 nm size) had a greater ability to induce apoptosis in the MC3T3-E1 cells than the other sized AgNP (50 nm and 100 nm).[47] It was shown that starch-capped AgNP had no effect on cancer cell lines U251 and fibroblasts IMR-90.[48]

Based on the bactericidal activity of the AgNP, a clinical bactericidal ultrasound gel containing 10 μg/mL was developed with a longer duration, compared with that of 5 μg/mL. A total of 50 specimens used commercial ultrasound gel (Figure 4A [L]) and 50 specimens, used self-prepared AgNP ultrasound gel (Figure 4A, [R]). The results indicated that bacterial contamination with *S. aureus* (ATCC 6538), *E. coli.* (ATCC 8099), *Pseudomonas aeruginosa.* (ATCC 15442), and *Candida albicans* (ATCC 10231) were found in all specimens using commercial gel, and no bacterial contamination was found from specimens using the self-prepared AgNP gel. Meanwhile, the image quality of ultrasound was evaluated in the preliminary trial, and the results demonstrated that there was no difference in the image quality between commercial gel

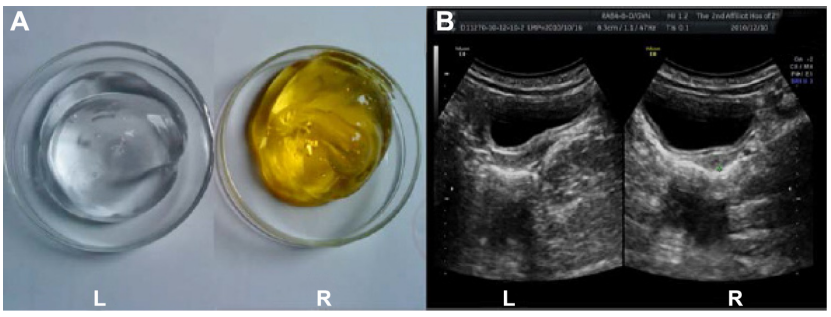

Figure 4 Photographs of ultrasound gel and examinations. Photographs of (**A**) ultrasound gel and (**B**) images of ultrasound examinations using commercial gel left (L) and the AgNP gel right (R).
Abbreviation: AgNP, silver nanoparticles.

and the self-prepared AgNP gel (Figure 4B). Also, there were not any noncompliance and adverse effects observed both during and after the experiments. We are carrying out a safety evaluation, including acute dermal toxicity test and an irritability test for further development of this product.

Conclusion

In this study, we developed a simple, green, and efficient route to synthesize AgNP by treating silver ions with CM extract at room temperature without using any harmful reducing, capping, or dispersing agents. CM extract plays an important role as the biofriendly reducing and stabilizing agent, reduces the cost of production, and the environmental impact. The prepared AgNP are spherical and single crystalline, with sizes in the range from 20 nm to 50 nm. Also, AgNP have effective growth-inhibition effects against *S. aureus* and *E. coli* and could be applied as clinical ultrasound gel without any noncompliance and adverse effects observed on the case samples.

Acknowledgments

This work was financially supported by National Natural Science Foundation of China (21272043, 81272452), the Science and Technology Planning Project of Guangdong Province (2007A020300007-10, 2011B090400573), Guangdong Natural Science Foundation (S2011010004967), and supported by the State Key Laboratory of Natural and Biomimetic Drugs (K20120204). This project was also supported by the Opening Project of Engineering Research Center of Cleaner Production in Chemical and Light Industry, Guangdong Higher Education Institutions, People's Republic of China.

Disclosure

The authors report no conflicts of interest in this work.

References

1. Tricoli A, Pratsinis SE. Dispersed nanoelectrode devices. *Nat Nanotechnol*. 2010;5(1):54–60.
2. Jin R, Cao YC, Hao E, Métraux GS, Schatz GC, Mirkin CA. Controlling anisotropic nanoparticle growth through plasmon excitation. *Nature*. 2003;425(6957):487–490.
3. Severin N, Kirstein S, Sokolov IM, Rabe JP. Rapid trench channeling of graphenes with catalytic silver nanoparticles. *Nano Lett*. 2009; 9(1):457–461.
4. Chen M, Yang Z, Wu H, Pan X, Xie X, Wu C. Antimicrobial activity and the mechanism of silver nanoparticle thermosensitive gel. *Int J Nanomedicine*. 2011;6:2873–2877.
5. Devi LS, Joshi SR. Antimicrobial and synergistic effects of silver nanoparticles synthesized using soil fungi of high altitudes of eastern Himalaya. *Mycobiology*. 2012;40(1):27–34.
6. Chladek G, Mertas A, Barszczewska-Rybarek I, et al. Antifungal activity of denture soft lining material modified by silver nanoparticles-a pilot study. *Int J Mol Sci*. 2011;12(7):4735–4744.
7. Martínez-Gutierrez F, Thi EP, Silverman JM, et al. Antibacterial activity, inflammatory response, coagulation, and cytotoxicity effects of silver nanoparticles. *Nanomedicine*. 2012;8(3):328–336.
8. Mohammed Fayaz A, Ao Z, Girilal M, et al. Inactivation of microbial infectiousness by silver nanoparticles-coated condom: a new approach to inhibit HIV- and HSV-transmitted infection. *Int J Nanomedicine*. 2012;7:5007–5018.
9. Kang K, Lim DH, Choi IH, et al. Vascular tube formation and angiogenesis induced by polyvinylpyrrolidone-coated silver nanoparticles. *Toxicol Lett*. 2011;205(3):227–234.
10. Ragaseema VM, Unnikrishnan S, Kalliyana Krishnan V, et al. The antithrombotic and antimicrobial properties of PEG-protected silver nanoparticle-coated surfaces. *Biomaterials*. 2012;33(11):3083–3092.
11. Prabakar K, Sivalingam P, Mohamed Rabeek SI, et al. Evaluation of antibacterial efficacy of phytofabricated silver nanoparticles using Mukia scabrella (Musumusukkai) against drug resistance nosocomial gram-negative bacterial pathogens. *Colloids Surf B Biointerfaces*. 2013;104:282–288.
12. Dar MA, Ingle A, Rai M. Enhanced antimicrobial activity of silver nanoparticles synthesized by Cryphonectria sp. evaluated singly and in combination with antibiotics. *Nanomedicine*. 2013;9(1):105–110.
13. Juan L, Zhimin Z, Anchun M, et al. Deposition of silver nanoparticles on titanium surface for antibacterial effect. *Int J Nanomedicine*. 2010; 15(5):261–267.
14. Tolaymat TM, El Badawy AM, Genaidy A, Scheckel KG, Luxton TP, Suidan M. An evidence-based environmental perspective of manufactured silver nanoparticle in syntheses and applications: a systematic review and critical appraisal of peer-reviewed scientific papers. *Sci Total Environ*. 2010;408(5):999–1006.
15. Kohl Y, Kaiser C, Bost W, et al. Preparation and biological evaluation of multifunctional PLGA-nanoparticles designed for photoacoustic imaging. *Nanomedicine*. 2011;7(2):228–237.
16. Godin B, Sakamoto JH, Serda RE, Grattoni A, Bouamrani A, Ferrari M. Emerging applications of nanomedicine for the diagnosis and treatment of cardiovascular diseases. *Trends Pharmacol Sci*. 2010; 31(5):199–205.
17. Tian J, Wong KK, Ho CM, et al. Topical delivery of silver nanoparticles promotes wound healing. *ChemMedChem*. 2007;2(1):129–136.
18. Meng H, Liong M, Xia T, et al. Engineered design of mesoporous silica nanoparticles to deliver doxorubicin and P-glycoprotein siRNA to overcome drug resistance in a cancer cell line. *ACS Nano*. 2010; 4(8):4539–4550.
19. El-Rafie MH, Shaheen TI, Mohamed AA, Hebeish A. Bionanoparticles and applications of silver nanoparticles onto cotton fabrics. *Carbohydr Polym*. 2012;90(2):915–920.
20. Dipankar C, Murugan S. The green synthesis, characterization, and evaluation of the biological activities of silver nanoparticles synthesized from Iresine herbstii leaf aqueous extracts. *Colloids Surf B Biointerfaces*. 2012;98:112–119.
21. Sivalingam P, Antony JJ, Siva D, Achiraman S, Anbarasu K. Mangrove Streptomyces sp. BDUKAS10 as nanofactory for fabrication of bactericidal silver nanoparticles. *Colloids Surf B Biointerfaces*. 2012;98:12–17.
22. Antony JJ, Sivalingam P, Siva D, et al. Comparative evaluation of antibacterial activity of silver nanoparticles synthesized using Rhizophora apiculata and glucose. *Colloids Surf B Biointerfaces*. 2011;88(1):134–140.
23. Niraimathi KL, Sudha V, Lavanya R, et al. Biosynthesis of silver nanoparticles using Alternanthera sessilis (Linn.) extract and their antimicrobial, antioxidant activities. *Colloids Surf B Biointerfaces*. 2013;102:288–291.
24. Kalimuthu K, Suresh Babu R, Venkataraman D, Bilal M, Gurunathan S. Biosynthesis of silver nanocrystals by Bacillus licheniformis. *Colloids Surf B Biointerfaces*. 2008;65(1):150–153.
25. Ingle A, Gade A, Pierrat S, Sonnichsen C, Rai M. Mycosynthesis of silver nanoparticles using the fungus Fusarium acuminatum and its activity against some human pathogenic bacteria. *Curr Nanosci*. 2008; 4(2):141–144.

26. Loo YY, Chieng BW, Nishibuchi M, Radu S. Synthesis of silver nanoparticles by using tea leaf extract from Camellia sinensis. *Int J Nanomedicine*. 2012;7:4263–4267.
27. Nabikhan A, Kandasamy K, Raj A, Alikunhi NM. Synthesis of antimicrobial silver nanoparticles by callus and leaf extracts from saltmarsh plant, Sesuvium portulacastrum L. *Colloids Surf B Biointerfaces*. 2010;79(2):488–493.
28. Venkatpurwar V, Pokharkar V. Green synthesis of silver nanoparticles using marine polysaccharide: study of in-vitro antibacterial activity. *Materials Letters*. 2011;65(6):999–1002.
29. Sun Xingyan, Sun Fengyi. *ShenNong's Herbal Classic*. 2010. Beijing. People's Medical Publishing House.
30. Ukiya M, Akihisa T, Yasukawa K, et al. Constituents of compositae plants. 2. Triterpene diols, triols, and their 3-o-fatty acid esters from edible chrysanthemum flower extract and their anti-inflammatory effects. *J Agri Food Chem*. 2001;49(7):3187–3197.
31. Lin GH, Lin L, Liang HW, et al. Antioxidant action of a Chrysanthemum morifolium extract protects rat brain against ischemia and reperfusion injury. *J Med Food*. 2010;13(2):306–311.
32. Jiang H, Xia Q, Xu W, Zheng M. Chrysanthemum morifolium attenuated the reduction of contraction of isolated rat heart and cardiomyocytes induced by ischemia/reperfusion. *Pharmazie*. 2004;59(7):565–567.
33. Miyazawa M, Hisama M. Antimutagenic activity of flavonoids from Chrysanthemum morifolium. *Biosci Biotechnol Biochem*. 2003;67(10):2091–2099.
34. Lee JS, Kim HJ, Lee YS. A new anti-HIV flavonoid glucuronide from Chrysanthemum morifolium. *Planta Med*. 2003;69(9):859–861.
35. Yen GC, Chen HY. Relationship between antimutagenic activity and major components of various teas. *Mutagenesis*. 1996;11(1):37–41.
36. Kurata R, Adachi M, Yamakawa O, Yoshimoto M. Growth suppression of human cancer cells by polyphenolics from sweet potato (Ipomoea batatas L.) leaves. *J Agric Food Chem*. 2007;55(1):185–190.
37. Hertog MG, Feskens EJ, Hollman PC, Katan MB, Kromhout D. Dietary antioxidant flavonoids and risk of coronary heart disease: the Zutphen Elderly Study. *Lancet*. 1993;342(8878):1007–1011.
38. Lai JP, Lim YH, Su J, Shen HM, Ong CN. Identification and characterization of major flavonoids and caffeoylquinic acids in three Compositae plants by LC/DAD–APCI/MS. *J Chromatogr B Analyt Technol Biomed Life Sci*. 2007;848(2):215–225.
39. Qin S, Wen X. Simultaneous determination of 6 active components in Chrysanthemum morifolium by HPLC. *Zhongguo Zhong Yao Za Zhi*. 2011;36(11):1474–1477. Chinese.
40. Wang YJ, Yang XW, Guo QS. Studies on chemical constituents in Huangjuhua (flowers of Chrysanthemum morifolium). *Zhongguo Zhong Yao Za Zhi*. 2008;33(5):526–530. Chinese.
41. Leroy S. Infectious risk of endovaginal and transrectal ultrasonography: systematic review and meta-analysis. *J Hosp Infect*. 2013;83(2):99–106.
42. Gray RA, Williams PL, Dubbins PA, Jenks PJ. Decontamination of transvaginal ultrasound probes: review of national practice and need for national guidelines. *Clin Radiol*. 2012;67(11):1069–1077.
43. Kora AJ, Manjusha R, Arunachalam J. Superior bactericidal activity of SDS capped silver nanoparticles: synthesis and characterization. *Mater Sci Eng C Mater Biol Appl*. 2009;29(7):2104–2109.
44. Babu SA, Prabu HG. Synthesis of AgNPs using the extract of Calotropis procera flower at room temperature. *Materials Letters*. 2011;65(11):1675–1677.
45. Carlson C, Hussain SM, Schrand AM, et al. Unique cellular interaction of silver nanoparticles: size-dependent generation of reactive oxygen species. *J Phys Chem B*. 2008;112(43):13608–13619.
46. Zhang FQ, She WJ, Fu YF. Comparison of the cytotoxicity in vitro among six types of nano-silver base inorganic antibacterial agents. *Zhonghua Kou Qiang Yi Xue Za Zhi*. 2005;40(6):504–507. Chinese.
47. Han DW, Woo YI, Lee MH, Lee JH, Lee J, Park JC. In-vivo and in-vitro biocompatibility evaluations of silver nanoparticles with antimicrobial activity. *J Nanosci Nanotechnol*. 2012;12(7):5205–5209.
48. Kim TH, Kim M, Park HS, Shin US, Gong MS, Kim HW. Size-dependent cellular toxicity of silver nanoparticles. *J Biomed Mater Res A*. 2012;100(4):1033–1043.
49. AshaRani PV, Low Kah Mun G, Hande MP, Valiyaveettil S. Cytotoxicity and genotoxicity of silver nanoparticles in human cells. *ACS Nano*. 2009;3(2):279–290.